

OPTIMAL FILTER DESIGN AND SWITCHING LOSS REDUCTION IN SINGLE PHASE GRID CONNECTED INVERTER SYSTEM

TONTEPU NAGA SOWMYA (109EE0052)

DEBATI MARANDI (109EE0280)



**Department of Electrical Engineering
National Institute of Technology Rourkela**

OPTIMAL FILTER DESIGN AND SWITCHING LOSS REDUCTION IN SINGLE PHASE GRID CONNECTED INVERTER SYSTEM

A Thesis submitted in partial fulfillment of the requirements for the degree of

Bachelor of Technology in “Electrical Engineering”

By

TONTEPU NAGA SOWMYA (109EE0052)

DEBATI MARANDI (109EE0280)

Under guidance of

Prof. B.CHITTI BABU



Department of Electrical Engineering
National Institute of Technology
Rourkela-769008 (ODISHA)
May-2013



DEPARTMENT OF ELECTRICAL ENGINEERING
NATIONAL INSTITUTE OF TECHNOLOGY, ROURKELA
ODISHA, INDIA-769008

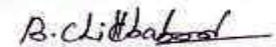
CERTIFICATE

This is to certify that the thesis entitled “**Optimal Filter design and Switching loss reduction in single phase grid connected inverter system**”, submitted by **Tontepu Naga Sowmya (Roll No.109EE0052) and Debati Marandi (Roll No. 109EE0280)** in partial fulfilment of the requirements for the award of **Bachelor of Technology in Electrical Engineering** during session 2012-2013 at National Institute of Technology, Rourkela. A bonafide record of research work carried out by them under my supervision and guidance.

The candidates have fulfilled all the prescribed requirements.

The thesis which is based on candidates’ own work, have not submitted elsewhere for a degree/diploma.

In my opinion, the thesis is of standard required for the award of a **bachelor of technology** degree in Electrical Engineering.



Dr. B.ChittiBabu
Supervisor
Dept. of Electrical Engineering
National institute of Technology
Rourkela-769008

ACKNOWLEDGEMENTS

This project is done as our final year project, as a part of course .We are really thankful to our project guide Prof. B Chitti Babu, Assistant Professor, Department of Electrical Engineering, for his invaluable guidance and assistance, without which the accomplishment of the task would have never been possible. He inspired us greatly to work in this project. His willingness to motivate us contributed tremendously to our project. We also would like to thank him for showing us some example that related to the topic of our project. We would also thank our friends who helped during our project.

Tontepu Naga Sowmya

Debati Marandi

B.Tech (Electrical Engineering)

Dedicated to

Our lovable parents and Friends...

ABSTRACT

With the reduction of available fossil fuels, the research in the area of renewable energy system has been exponentially increased in order to find out an effective solution. Considering the case of a PV panel, it is observed that it produces a DC voltage which has to be converted to AC for grid connected applications. So a Voltage Source Inverter (VSI) with a PWM control of switching action is used for this purpose.

This project presents the comparative study between unipolar and bi-polar switching scheme for single-phase grid-connected inverter system with filter design on the grid side. For that, LCL filter is considered and its performance for current ripple reduction on grid-side is compared with normal L and LC filter. It is seen that the response for LCL filter show the best results with lower current ripple as compared to L and LC Filter. Further, the obtained results show that the obtained LCL-filter can provide sufficient attenuation of current harmonics and mean while injects a sinusoidal current into the grid for maintaining power quality standard. In addition to that, the method to design the inductor is also studied.

Further, the optimal design of LCL filter for grid connected inverter system is studied. For that, initially normal design is considered. Then the conduction and switching losses that are caused by the filter are calculated and are optimized considering the level of reduction of harmonics. Hence the main aim of the study is to attenuate higher order harmonics along with the reduction in switching losses to ensure sinusoidal current injection into the grid. Further, the different switching schemes for single phase unipolar full bridge inverter are studied and compared to get the switching scheme which gives lesser switching losses. The LCL filter is designed accordingly and optimal inductance and capacitance values are obtained. The complete model of the study is simulated in MATLAB-Simulink environment for feasibility of the study.

CONTENTS

Abstract	v
Contents	vii
List of Figures	ix
List of Tables	x
Abbreviations and Acronyms	xi

CHAPTER 1

INTRODUCTION

1.1 Motivation	2
1.2 Introduction	2
1.3 Literature review	4
1.4 Organization of thesis	4

CHAPTER 2

MATHEMATICAL MODELLING OF SINGLE PHASE VOLTAGE SOURCE INVERTER

2.1 Mathematical modeling of an inverter	
2.1.1 Unipolar Switching Control	7
2.1.2 Bipolar Switching Control	11

CHAPTER 3

LCL FILTER DESIGN

3.1 Types of filter	14
3.2 LCL filter with passive damping	14
3.3 Optimal LCL filter design	15

CHAPTER 4

SWITCHING LOSS REDUCTION WITH LCL FILTER

4.1 Different switching methods	20
4.2 Reduction of switching losses	21

CHAPTER 5

SIMULATION RESULTS AND DISCUSSIONS	23
---	----

CHAPTER 6

CONCLUSION AND FUTURE WORK

6.1 Conclusion	30
6.2 Future Work	30
References	31
Appendix	
a) Small signal analysis of single phase inverter	34
b) Inductor design of the filter	37
Publication(s)	39

LIST OF FIGURES

Fig.1.1. Single phase grid connected inverter with LCL filter.	(3)
Fig.2.1. Shows the topology for single phase full bridge inverter	(7)
Fig.2.2. Output voltage and current waveform of unipolar switching scheme inverters	(8)
Fig.2.3. Magnitude distribution of Δi_{pp} unipolar switching scheme for $\mu=0.8$	(9)
Fig .2.4. Typical filter inductor ripple current of ΔI of single-phase full-bridge inverter when $\mu=0.8$.	(9)
Fig .2.5. RMS calculation of the equivalent of filter inductor ripple current Δi	(10)
Fig.2.6. Output voltage and current waveform of bipolar switching scheme inverters	(11)
Fig.2.7. Magnitude distribution of Δi_{pp} bipolar switching scheme for $\mu=0.8$	(11)
Fig.2.8 Response of typical filter inductor ripple current of ΔI of single-phase half-bridge inverter when $\mu = 0.8$	(12)
Fig.3.1. LCL filter design with passive damping	(16)
Fig.3.2. Variation of Q-factor in terms of a_c	(17)
Fig.5.1 Variation of total power losses with L in p.u	(25)
Fig.5.2. Normalised switching frequency	(27)
Fig.5.3. Normalised switching frequency at $\phi = \frac{\pi}{6}$	(27)
Fig.5.4. Switching loss and their average values for a cycle	(28)
Fig.5.5. Switching loss and their average values at $\phi = \frac{\pi}{6}$	(28)
Fig.A.1. when S1 and S2 switches are ON	(34)
Fig.A.2. when switches S3 and S4 are ON	(35)
Fig.A.3. small signal model	(36)

LIST OF TABLES

TABLE-5.1. DESIGN PARAMETERS	(24)
TABLE-5.2. FILTER VALUES AND THD% FOR UNIPOLAR SWITCHING SCHEME	(24)
TABLE-5.3. FILTER INDUCTANCE VALUE AND THD% FOR BI-POLAR SWITCHING SCHEME	(24)
TABLE-5.4.: POWER LOSSES IN FILTER	(25)
TABLE 5.5.TOTAL LOSSES WITH THD% VARIATION	(26)

ABBREVIATIONS AND ACRONYMS

THD – Total Harmonic Distortion

PWM – Pulse Width Modulation

VSI – Voltage Source Inverter

RMS – Root Mean Square

CHAPTER 1

Introduction

1.1 MOTIVATION:

For past couple of decades, energy demand has increased dramatically and also amount of fossil fuels has been depleting to a minimum extent. In addition to that environmental pollution has also been increased due to CO₂ emissions from the conventional power plants namely: thermal and nuclear plants. As a result, non conventional energy sources of energy such as solar, wind, and geothermal have gained popularity now a days. But the conversion efficiency of these sources is very less which leads to a very high cost of production. Taking the case of a photo-voltaic system, the cost of PV panel is very high and at the same time the energy conversion is 15-20%. In addition to that there are losses that further occur in converting the current so that it can be fed to the grid. Also during this conversion process, an inverter that is used to convert DC to AC introduces harmonics to the grid side current which may lead to the damage of the load. So, design of a filter is necessary to remove these harmonics. Also, power loss reduction is needed to improve the efficiency of the system.

1.2 INTRODUCTION:

The key issues like future energy demand, environmental problems and depletion of fossil fuels have become Global Issue at present scenario. There are different schedules to provide solution to these problems. Short term energy schedule and Mid-term energy schedule are to save and use the energy efficiently. But our goal is to provide solution for a long term. The long term energy schedule is to produce energy by using renewable energy sources such as wind, solar, fuel cell etc [1]. Renewable energies are clean and green energies. It depends upon the sources e.g. more wind power can be extracted when there is continuous and strong blow of wind and solar energy is extracted more during midday. As a result, this type of dispersed power generating system causes the power quality problems to the utility grid. Power electronics converter is key component to interface renewable energy source (RES) with utility grid to satisfy the grid code requirements [2]. Hence these converters are usually connected to the grid through a simple L filter to reduce the AC side current harmonic, in order to meet corresponding harmonic standards, however, a larger volume of inductance result in deterioration of system dynamic response cost. Also such a filter is bulky, inefficient and cannot meet the regulatory requirements regarding interconnection of harmonic loads to grid [3].

The grid interfacing converters are basically power electronic converters acts as an interface between electrical load and distributed generation to the grid. This inverter match the characteristics of renewable energy source and the requirements of the grid connections, provides the DPGS with power system control capabilities, improves power quality and their effect on power system stability [9]. However, due to non-linear switching characteristics of inverter switches, the grid current waveform contains higher order harmonics A filter connected in series with the inverter makes sure that the harmonic content is below the specified limit.

There are different kinds of filters like L, LC and LCL are extensively studied in the available literature. Among all of them, LCL filter is proved to have better harmonic attenuation for the same value of inductance [10]. The resonance problem in the filter is overcome by using different damping methods. The LCL filter is connected in series with the inverter on the output side. The schematic diagram of single-phase grid connected inverter is shown in Fig.1.1 with incorporation of LCL filter on grid side.

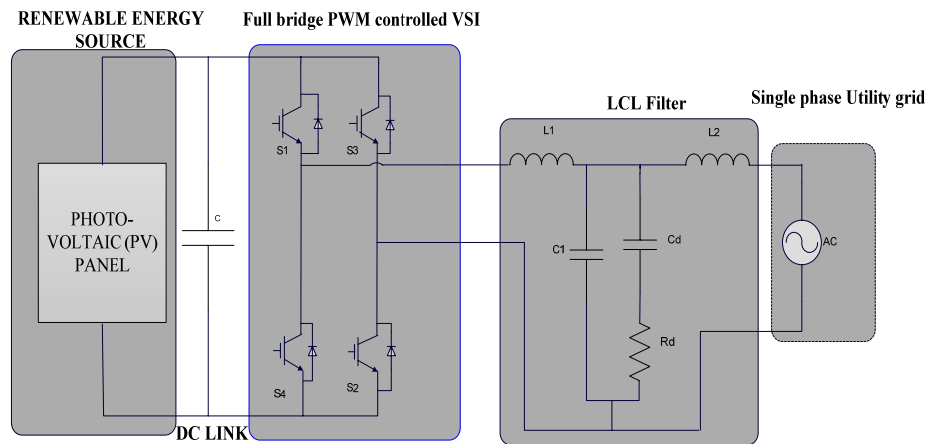


Fig.1.1. Single phase grid connected inverter with LCL filter

In this project optimal design of LCL filter for grid connected inverter system is also studied. Here, initially normal design is studied. Then the conduction and switching losses that are caused by the filter are calculated and are optimized considering the level of reduction of harmonics. Hence our main aim is to attenuate harmonics along with the reduction in switching losses. Also different switching schemes for single phase unipolar full bridge inverter are studied and compared to get the switching scheme which gives lesser switching losses. The LCL filter is

designed accordingly and optimal inductance and capacitance values are obtained. All the related models are simulated using the MATLAB software and graphs are studied.

1.3 LITERATURE REVIEW:

The importance of renewable energy sources is given by [1]. The paper [3] gave the initial idea of filter of why it is used how it is to be connected. Then the further study continued when the more about single phase inverters is studied in [5]. Reference [4]-[7] aided in the comparative study between unipolar and bipolar switching schemes and also in the study where LCL filter is proved to be a better one in attenuating higher order harmonics. Later in this work, the filter design is optimized by following the work of [11] taking the losses caused by the filter. Further research continued to reduce the switching loss of the inverter [12] so that the efficiency of the whole system is increased. One can reduce the switching losses by simply applying soft switching scheme but the external components that are used are sometimes of higher rating than that of the switches of the inverter and hence soft switching is not a better option. It is important that the inverter supplies appropriate voltage and frequency waveform in island mode. The voltage must comply with amplitude and frequency conditions regardless of the type of load connected. In order to study the stability of the system, transfer function is found out by making small signal analysis [15].

1.4 ORGANIZATION OF THESIS:

The thesis is organized as follows. Chapter 1 presents the introduction about the project followed by the thesis objectives.

Chapter 2 deals with Mathematical modelling of the inverter so that the peak to peak current and the RMS current on the output side of the inverter can be calculated. Also different inverters like full bridge inverter with unipolar switching scheme and half bridge inverter with bipolar switching scheme are compared with their respective output current harmonics present in order to find out which one is better suitable for grid connected applications.

Chapter 3 includes the filter design. Initially different types of filters with their drawbacks that lead to the introduction of the next one are studied and then, the final LCL filter

is designed. Then the damping methods to reduce the resonance effect caused in the filter are studied. And then the final optimal filter design which gives lower losses at the THD% which is accepted by Grid code requirements is designed.

Chapter 4 discusses different switching schemes and the scheme that provides lesser losses is studied. Then the switching frequency waveform and the losses curve are plotted to compare with the other methods.

Chapter 5 presents the different output waveforms and graphs. Initially the current waveforms are studied and then the losses and the THD% graph to optimize the filter design are plotted and then switching frequency and losses graphs are plotted and then analyzed.

Chapter 6 provides the conclusions that derived from the whole project. It shows which control action is to be selected and what filter is to be selected and the damping method that suits the required needs is found out. Then the future work is discussed.

CHAPTER 2

Mathematical Modelling of Single Phase Voltage Source Inverter

2.1 MATHEMATICAL MODELLING:

2.1.1 Unipolar Switching Scheme:

The schematic diagram of full bridge inverter topology is illustrated in Fig.2.1 The grid voltage is assumed to be sinusoidal. Thus the fundamental component is shown by

$$v = v_0 - e = 0 \quad (2.1)$$

The full bridge topology shows us the unipolar switching action, the output is either high to zero or low to zero, rather than high to low as shown in Fig 2.2.

S_1 is on when $v_{\sin e} > v_{tri}$

S_2 is on when $-v_{\sin e} < v_{tri}$

S_3 is on when $v_{\sin e} > v_{tri}$

S_4 is on when $-v_{\sin e} < v_{tri}$

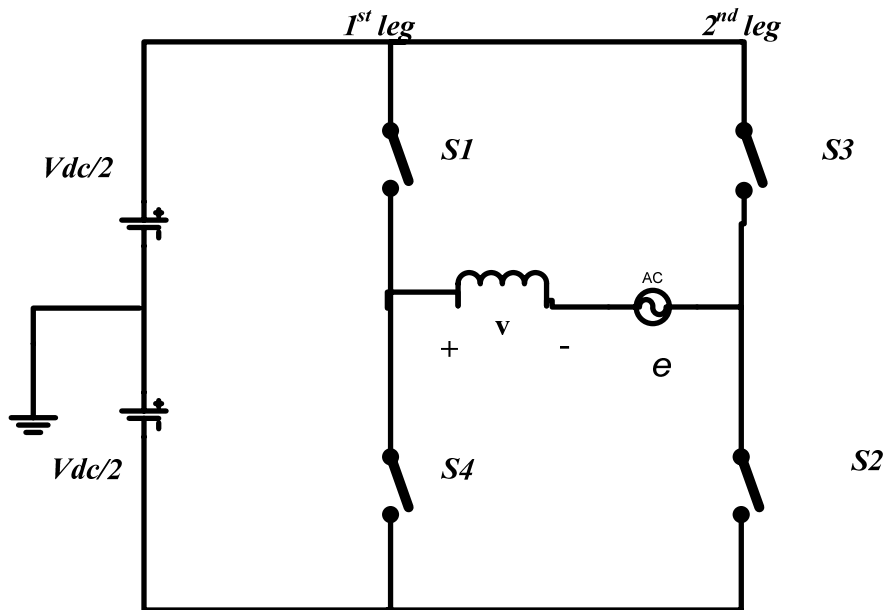


Fig.2.1. Shows the topology for single phase full bridge inverter

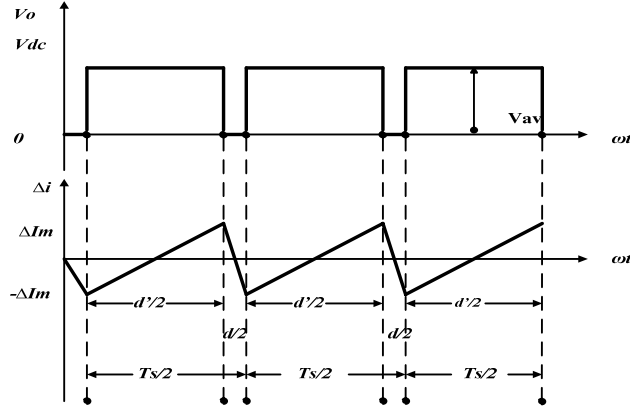


Fig.2.2 Output voltage and current waveform of unipolar switching scheme inverters.

In this reference, analyzes of switching ripple current on the grid-side filter is presented here

a. Calculation of ripple current and its RMS value

When the switching frequency f_{sw} is higher than the operating frequency f_o , then the inverter output is regarded to be constant during the switching interval T_s . Therefore, the filter inductor current is found to be a triangular waveform as shown in Fig.2.2 (a) for full-bridge topology. The inductor for unipolar PWM can be measured by

$$L \frac{2\Delta i_{max}}{ontime} = V_{dc} - V_{av} \quad (2.2)$$

$$ontime = \frac{d'}{2} T_s \quad (2.3)$$

$$i_{pp} = 2\Delta i_{max} = \frac{(V_{dc} - V_{av})}{L} \frac{d'}{2} T_s \quad (2.4)$$

Replacing the above equation with the following three equations:

$$e(\omega t) = \mu V_{dc} \sin(\omega t), \quad (2.5)$$

$$V_{av}(\omega t) = d_1(\omega t) V_{dc}, \quad (2.6)$$

$$d'(\omega t) = \mu \sin(\omega t), \text{ for } 0 < \omega t < \pi \tag{2.7}$$

where μ is the modulation index.

Therefore the equation changes to,

$$\Delta i_{pp}(\omega t) = \frac{V_{dc} T_s}{2L} (1 - \mu \sin(\omega t)) \mu \sin(\omega t) \tag{2.8}$$

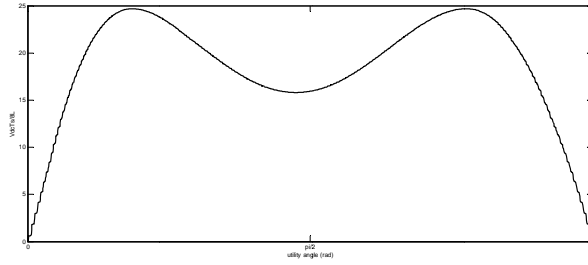


Fig.2.3. Magnitude distribution of Δi_{pp} unipolar switching scheme for $\mu = 0.8$

Fig.2.3. shows the magnitude distribution of Δi_{pp} for unipolar switching scheme. Since, the voltage and current waveforms are half-wave symmetry, the situation during $\pi < \omega t < 2\pi$ repeats same as that of during $0 < \omega t < \pi$ [5]. The ripple current consisted of several triangular waves bounded by $\pm \Delta i_{pp} / 2$ as depicted in Fig.2.4. The corresponding RMS calculation of switching current ripple for filter design is shown in Fig.2.5.

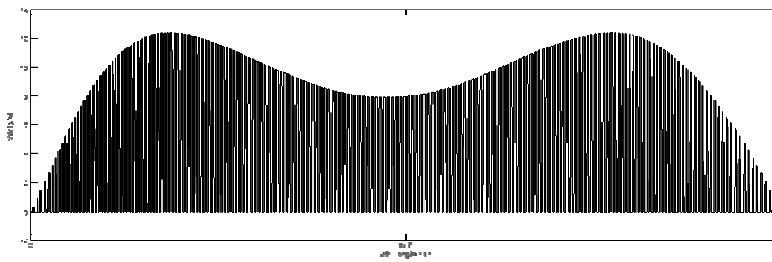


Fig .2.4. Typical filter inductor ripple current of Δi of single-phase full-bridge inverter when $\mu = 0.8$.

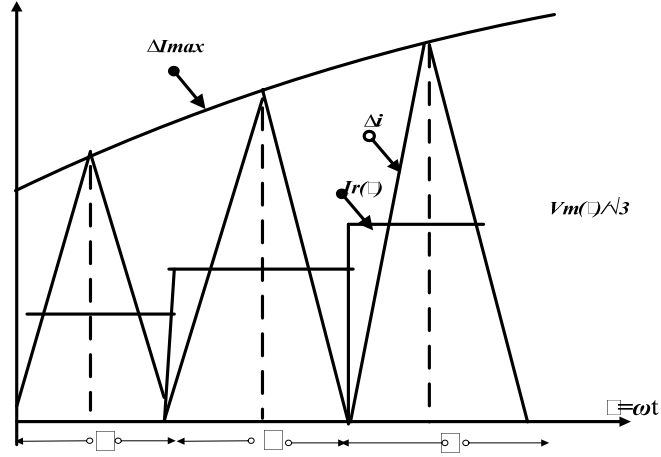


Fig .2.5. RMS calculation of the equivalent of filter inductor ripple current Δi

From that,

$$\Delta I_{\max}(\theta_k) = \frac{V_{dc}T_s}{4L} [1 - \mu \sin(\theta_k)] \mu \sin(\theta_k) \quad (2.9)$$

Here $\theta_k = \frac{(2k-1)\pi}{4n}$, $k=1,2,\dots,n$. Since, the RMS value of triangular wave is $\Delta I_{\max} / \sqrt{3}$ as shown Fig .2.5, therefore the RMS value of the ripple current can be calculated by

$$I_r = \sqrt{\frac{2}{3\pi} \int_0^{\pi/2} \Delta I_{\max}^2(\theta) d\theta} \quad (2.10)$$

Now, substituting equation (2.9) in equation (2.10) we get,

$$\begin{aligned} I_r &= \frac{V_{dc}T_s}{4L} \mu \sqrt{\frac{2}{3\pi} \int_0^{\pi/2} (1 - \mu \sin \theta)^2 \sin^2 \theta d\theta} \\ &= \frac{V_{dc}T_s}{4L} \mu \sqrt{\frac{2}{3\pi} \left[\frac{\pi}{4} \left(1 + \frac{3}{4} \mu^2 \right) - \frac{4}{3} \mu \right]} \end{aligned} \quad (2.11)$$

2.1.2 Bipolar Switching Scheme:

The topology of bridge that is shown in fig.2.1 can also be used as a half bridge topology if the second leg of the full bridge is not used and the node is directly connected to the split of the DC source near the ground [4].

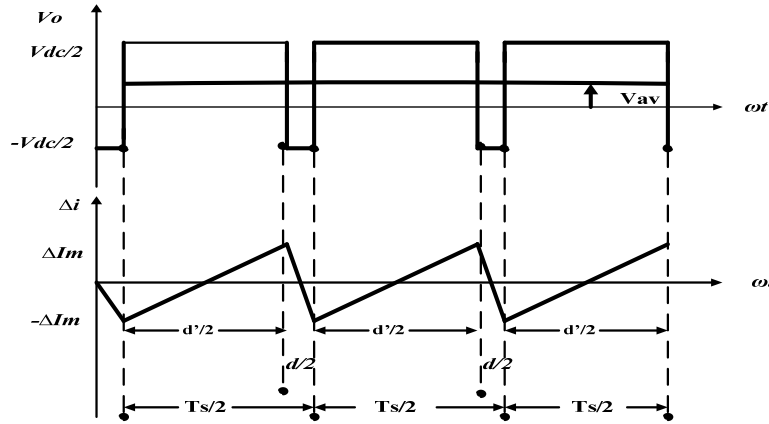


Fig.2.6. Output voltage and current waveform of bipolar switching scheme inverters

Fig.2.6 illustrates the principle of sinusoidal bipolar PWM using half bridge inverter topology. When the instantaneous value of the sine reference is larger than the triangular carrier signal, the output is at $+V_{dc}/2$ and $-V_{dc}/2$ for vice-versa.

The filter inductor current is found to be a triangular waveform as shown in Fig.2.6. for a bipolar switching action.

Therefore the peak to peak current can be derived similar to that of unipolar switching just by replacing V_{dc} by $V_{dc} / 2$. And it is calculated to be

$$\Delta i_{pp}(\omega t) = \frac{V_{dc} T_s}{4L} \{1 - \mu^2 \sin^2(\omega t)\} \quad (2.12)$$

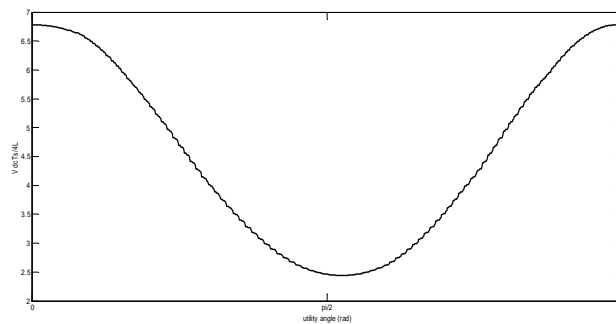


Fig.2.7. Magnitude distribution of Δi_{pp} bipolar switching scheme for $\mu=0.8$

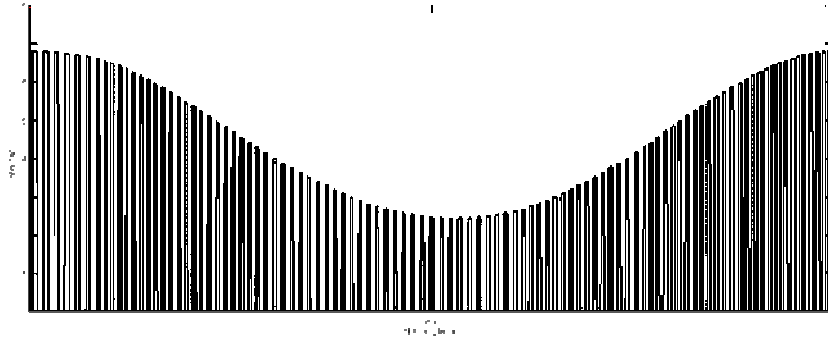


Fig.2.8 Response of typical filter inductor ripple current of ΔI of single-phase half-bridge inverter when $\mu = 0.8$

RMS value of the switching ripple current in half-bridge inverters can be calculated as it is calculated for unipolar switching and it is found out to be

$$I_r = \frac{V_{dc} T_s}{8L} \sqrt{\frac{1}{3} \left[\left(1 - \mu^2 + \frac{3}{8} \mu^4 \right) \right]} \quad (2.13)$$

CHAPTER 3

LCL Filter design

3.1 Types of filter:

3.1.1 L filters:

Firstly an L filter is a simple filter designed to mitigate the harmonics in the grid side current. But there are many drawbacks of L filter like poor system dynamics, low attenuation and long time response. In order to improve the mitigation level, we have to either increase the value of the inductor or increase switching frequency where both of them cause increased losses.

3.1.2 LC filters:

A shunt element is added to an L filter to improve the attenuation of the switching frequency components. Since a capacitance gives low reactance at the high switching frequency it is selected as the shunt element. But it is observed that the load impedance across the capacitor is very high.

3.1.3 LCL filters:

It provides better decoupling between the filter and the grid impedance. It also has better attenuation ratio with smaller values of L and C. Hence LCL filter is designed for grid connected applications. Resonance is the main problem with LCL filter and it can be damped either by using active damping methods or passive damping methods. But for grid connected applications passive damping method is necessary in case when inverter is switched off and filter is still connected to the grid.

3.2 LCL filter design with passive damping

Here a resistor is connected in series with the capacitor as a part of passive damping scheme. Table-1 shows the details of the data used for calculation of filter inductor value [6].

$$I_1 = \frac{\mu V_{dc}}{\sqrt{2} Z_{base}} = \frac{\mu V_{dc}}{2\pi\sqrt{2}L_b} \quad (3.1)$$

Therefore, the switching ripple for full-bridge topology can be calculated by

$$RF_{sw} = \frac{I_r}{I_1} = \frac{V_{dc}T_s}{4L} \mu \sqrt{\frac{2}{3\pi} \left[\frac{\pi}{4} \left(1 + \frac{3}{4}\mu^2 \right) - \frac{4}{3}\mu \right]} \frac{2\pi\sqrt{2}}{\mu V_{dc}T} L_b$$

$$\frac{L}{L_b} \geq \frac{1}{RF_{sw}} \sqrt{\frac{\pi}{3} \left[\frac{\pi}{4} \left(1 + \frac{3}{4} \mu^2 \right) - \frac{4}{3} \mu \right]} \frac{T_s}{T} \quad (3.2)$$

For half-bridge topology switching ripple current can be calculated as

$$RF_{sw} = \frac{I_r}{I_1} = \frac{V_{dc} T_s}{8L} \sqrt{\frac{1}{3} \left(1 - \mu^2 + \frac{3}{8} \mu^4 \right)} \frac{4\pi\sqrt{2}}{\mu V_{dc} T} L_b \quad (3.3)$$

$$\frac{L}{L_b} \geq \frac{1}{RF_{sw}} \sqrt{\frac{\pi^2 (1 - \mu^2 + 3\mu^2 / 8)}{6\mu^2}} \frac{T_s}{T} \quad (3.4)$$

where, $Z_{base} = \frac{V^2}{P}$ and $L_b = \frac{Z_{base}}{2\pi f_o}$

The resonant frequency should be in the range $10 \omega_o < \omega_{res} < (\omega_{sw}/2)$ which is an important condition for filter inductor design. Table-5.2 and Table-5.3 gives the typical filter with their % THD values of grid currents.

$$C_f = \frac{Q_{re}}{\omega_o V^2} = \frac{\alpha P}{\omega_o V^2} \quad \alpha = 2.5\% P \quad (3.5)$$

$$R = \frac{1}{3\omega_{res} C_f} \quad (3.6)$$

3.3 Optimal LCL Filter design

The design of the LCL filter should also consider the selection of resonance frequency (ω_{res}). The resonance frequency depends upon the circuit elements. So, the resonance frequency range to be selected to avoid resonance problems,

$$10\omega_0 \leq \omega_{res} \leq \frac{\omega_{sw}}{2} \quad (3.7)$$

Where, ω_0 is utility frequency and ω_{sw} is switching frequency.

Passive damping is adopted for grid connected applications since when inverter is switched off still there will be a capacitor to provide the continuity of supply.

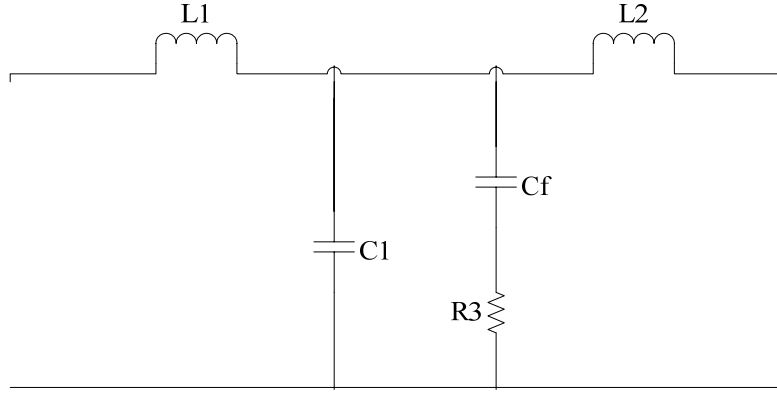


Fig.3.1.LCL filter design with passive damping

Resonance frequency is given by the equation,

$$\omega_r^2 = \frac{1}{LC} \quad (3.8)$$

Where $L = L_1 + L_2$ and $C = C_1 + C_f$

The relation between L_1 and L_2 is given by $L_1 = a_L L_2$ and between C_1 and C_f is given by $C_f = a_C C_1$

Determination of a_L and a_C :

- 1) Generally L_1 and L_2 remains same and hence $a_L = 1$
- 2) The selection of a_C is tradeoff between effective damping and power loss in shunt damping circuit. So, to get a_C we use the following transfer function,

$$\frac{u_2(j\omega)}{u_i(j\omega)} = \frac{0.5 + 0.5C_f R_3 j\omega}{(1 - \frac{\omega^2}{\omega_r^2}) + j\omega C_f R_3 (1 - \frac{\omega^2}{\omega_r^2} \frac{1}{1 + a_C})} \quad (3.9)$$

To find the Q-factor,

$$\lim_{\omega \rightarrow 0} \left| \frac{u_c}{u_i} \right| = 0.5 \quad (3.10)$$

$$\left| \frac{u_c}{u_i} \right|_{\omega = \omega_r} = \left| \frac{0.5 + j0.5\omega_r C_f R_3}{j\omega_r C_f R_3 \frac{a_C}{1 + a_C}} \right| \quad (3.11)$$

Dividing (3.11) by (3.10) we get,

$$Q(a_c) = \frac{\left| 1 + j\omega_r C_f R_3 \frac{a_c}{1 + a_c} \right|}{\left| j\omega_r C_f R_3 \frac{a_c^2}{(1 + a_c)^2} \right|} \quad (3.12)$$

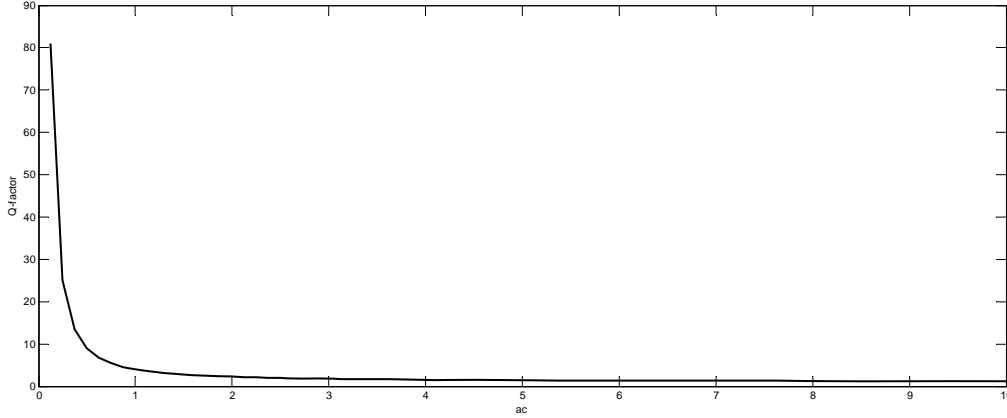


Fig.3.2.Variation of Q-factor in terms of a_c

Losses increases with increase in a_c and hence the optimal value of a_c is found out to be 1 as studied in [10]

3.3.1 Power losses in the damping Circuit:

The power loss in the damping circuit is calculated as shown below. The losses at switching frequency and fundamental frequency are only calculated because other harmonics do not contribute much to the losses. Power losses are calculated for p.u. and then actual values are calculated for a given base value.

i) Fundamental frequency power loss:

$$P_{d(50)} = \text{Real}[U_c I_d^*] \quad (3.13)$$

$$I_d = U_c \frac{sC_f}{1 + sC_f R_3} \quad (3.14)$$

$$I_d = U_c \frac{j\omega_{50} C_f (1 - j\omega_{50} C_f R_3)}{1 + \omega_{50}^2 C_f^2 R_3^2} \quad (3.15)$$

$$P_{d(50)} = \frac{U_c^2 \omega_{50}^2 C_f^2 R_3}{1 + \omega_{50}^2 C_f^2 R_3^2} \quad (3.16)$$

Where ω_{50} is fundamental frequency in p.u.(rad/sec), U_c is 1 p.u.

ii) Switching frequency power loss:

Grid is considered as a short circuit at the switching frequency but it is an ideal voltage at fundamental frequency. So at switching frequency $U_g=0$,

$$U_c = U_i \frac{0.5 + j0.5\omega_{sw}C_fR_3}{(1 - \frac{\omega_{sw}^2}{\omega_r^2}) + j\omega_{sw}C_fR_3(1 - \frac{\omega_{sw}^2}{\omega_r^2} \frac{1}{1+a_c})} \quad (3.17)$$

$$I_d = U_c \frac{\omega_{sw}C_f(\omega_{sw}C_fR_3 + j)}{1 + \omega_{sw}^2C_f^2R_3^2} \quad (3.18)$$

$$P_{d(sw)} = \text{Real}[U_c I_d^*] \quad (3.19)$$

Representing U_c and I_d as complex fractions,

$$U_c = U_i \frac{a + jb}{c + jd} \quad (3.20)$$

$$I_d = U_c \frac{\omega_{sw}C_d}{1 + \omega_{sw}^2C_d^2R_d^2} (x + jy) \quad (3.21)$$

$$U_c I_d^* = U_i \frac{a + jb}{c + jd} U_i \left(\frac{a + jb}{c + jd}\right)^* \frac{\omega_{sw}C_f}{1 + \omega_{sw}^2C_f^2R_3^2} (x + jy)^* \quad (3.22)$$

$$P_{d(sw)} = \text{Real}[U_c I_d^*] = U_i \frac{2a^2 + b^2}{c^2 + d^2} \frac{\omega_{sw}C_f}{1 + \omega_{sw}^2C_f^2R_3^2} x \quad (3.23)$$

Here,

$$a = 0.5, \quad b = 0.5\omega_{sw}c_fR_3, \quad c = 1 - \frac{\omega_{sw}^2}{\omega_r^2}, \quad d = \omega_{sw}C_fR_3 \left(1 - \frac{\omega_{sw}^2}{\omega_r^2} \frac{1}{1+a_c}\right), \quad x = \omega_{sw}C_fR_3, \quad y = 1$$

3.3.2 Power losses in the inductor:

The power losses in the inductor are calculated using the software called Magnetic design where the inputs given are inductor value, peak to peak current and RMS current of the ripple.

CHAPTER 4

Switching loss reduction with LCL filter

4.1 DIFFERENT SWITCHING METHODS:

One more losses that has major contribution to the losses in the inverter system is Switching losses of the switches used in the system. Three different methods are studied to reduce the losses and the one that is giving lower switching losses is selected. The equations are adopted from [13]

The switching loss for one cycle is assumed to be directly proportional to current [12].

Therefore, the average switching loss per cycle can be calculated as

$$q_{sub}(\omega t) = \frac{K|i_1(\omega t)|}{T_s(\omega t)} \quad (4.1)$$

Where K is a constant that depends upon DC voltage, i_1 is instantaneous current and T_s is switching period. Since, we are going to vary switching frequency in different methods, here $T_s(\omega t)$ is taken as a function.

The switching losses can be given as

$$q_{sub}(\omega t) = \frac{K\sqrt{2}I_1|\sin(\omega t - \phi)|}{T_s(\omega t)} \quad (4.2)$$

Where ϕ is the lagging angle of the grid current.

The average switching losses for a cycle can be derived as follows,

$$Q(T_s(\omega t)) = \frac{1}{\pi} \int_0^{\pi} q_{sub}(\omega t) d\omega t \quad (4.3)$$

$$= \frac{K\sqrt{2}I_1}{\pi} \int_0^{\pi} \frac{|\sin(\omega t - \phi)|}{T_s(\omega t)} d\omega t \quad (4.4)$$

4.1.1 Constant switching frequency:

In this case we take constant switching frequency. Therefore T_s (ωt) remains constant. The switching losses graph would be a sinusoidal plot.

$$q(T_s(\omega t)) = \frac{K\sqrt{2}I_1}{T_s} |\sin(\omega t - \phi)| \quad (4.5)$$

a. Constant ripple scheme:

In this case we take constant required rms current ripple. From that value peak to peak ripple is calculated,

$$\Delta I_{pk-pk} = 2\sqrt{3}\Delta I_{rms,req} \quad (4.6)$$

We know that ΔI_{pk-pk} as derived in [14]

$$\Delta i_{pp}(\omega t) = \frac{V_{dc}T_s}{2L}(1 - m_a \sin(\omega t)) \cdot m_a \sin(\omega t) \quad (4.7)$$

Hence $T_s(\omega t)$ is derived from above equation,

$$T_s(\omega t) = \frac{2\sqrt{3}\Delta I_{rms,req}L}{V_d(1 - m_a |\sin \omega t|)m_a |\sin \omega t|} \quad (4.8)$$

Therefore,

$$q(T_s(\omega t)) = \frac{K\sqrt{2}I_1V_d}{2\sqrt{3}\Delta I_{rms,req}L} |\sin(\omega t - \phi)| |1 - m_a \sin \omega t| m_a \sin \omega t \quad (4.9)$$

4.2 REDUCTION OF SWITCHING LOSSES

4.2.1 Optimal Switching scheme:

In this method, the value or function of $T_s(\omega t)$ is selected such that the switching losses are lower. As derived in [11],

$$T_s(\omega t) = C' \left(\frac{|\sin(\omega t - \phi)|}{(1 - m_a |\sin \omega t|)^2 (m_a \sin \omega t)^2} \right)^{\frac{1}{3}} \quad (4.10)$$

Where,

$$C' = \frac{2\sqrt{3}\Delta I_{rms,req} L}{V_d m_a \sqrt{\frac{1}{\pi} \int_0^\pi \{[\sin(\omega t - \phi)]^2 (1 - m_a \sin \omega t)^2 (\sin \omega t)^2\}^{\frac{1}{3}} d\omega t}} \quad (4.11)$$

Substituting the above function of $T_s(\omega t)$ in $q_{sub}(\omega t)$ we get the expression for switching loss,

$$q(T_s(\omega t)) = \frac{K\sqrt{2}I_1 |\sin(\omega t - \phi)|^{\frac{2}{3}} |1 - m_a \sin \omega t|^{\frac{2}{3}} |m_a \sin \omega t|^{\frac{2}{3}}}{C'} \quad (4.12)$$

CHAPTER 5

Simulation Results and Discussions

TABLE-5.1. DESIGN PARAMETERS

Parameters	Value
Rated power P	1 KVA
Rated voltage V	230 V
Operating frequency f_o	50 Hz
Switching frequency f_{sw}	5 KHz

TABLE-5.2. FILTER VALUES AND THD% FOR UNIPOLAR SWITCHING SCHEME

Filter	L	LC	LCL
Inductance	1.475mH	1.475mH	$L_1=1.028\text{mH}$ $L_2=0.4469\text{mH}$
Capacitance	-	$16.44 \mu F$	$16.44 \mu F$
Resistance	-	-	3.15Ω
THD%	5.95	1.58	0.7

TABLE-5.3. FILTER INDUCTANCE VALUE AND THD% FOR BI-POLAR SWITCHING SCHEME

Filter	L	LC	LCL
Inductance	0.405mH	0.405mH	$L_1=0.2833\text{mH}$ $L_2=0.1232\text{mH}$
Capacitance	-	$16.44 \mu F$	$16.44 \mu F$
Resistance	-	-	1.65Ω
THD%	6.08	2.7	1.5

From the above tables it is observed that for the same value of inductance L filter offers lower attenuation whereas LCL offers better mitigation than that of L and LC. Also when unipolar and bipolar switching schemes are compared, for the same filter connected on the grid side of the inverter, it is proved that Unipolar has better attenuation because it has four switches. But at the same time it has higher switching losses because it has more number of switching than that of bipolar which has only two switches. These losses are compensated by better THD%. Hence it is obtained that unipolar switching with LCL filter is better for and Grid connected applications and further research is continued taking them.

TABLE-5.4.: POWER LOSSES IN FILTER

Inductance (L) in p.u.	Total losses at fundamental frequency(50Hz)	Total losses at switching frequency (5 kHz)	Total losses in capacitor (C1) and damping circuit
0.01	0.4650	0.2575	64.5410
0.02	0.6540	0.1235	32.2270
0.03	0.9470	0.0815	21.4847
0.04	1.1780	0.0645	16.1135
0.05	1.2880	0.0505	12.8900
0.06	1.4540	0.0425	10.7400
0.07	2.0750	0.0385	9.2070
0.08	2.1380	0.0335	8.0500
0.09	1.8970	0.0305	7.1650
0.1	2.1320	0.0255	6.4400

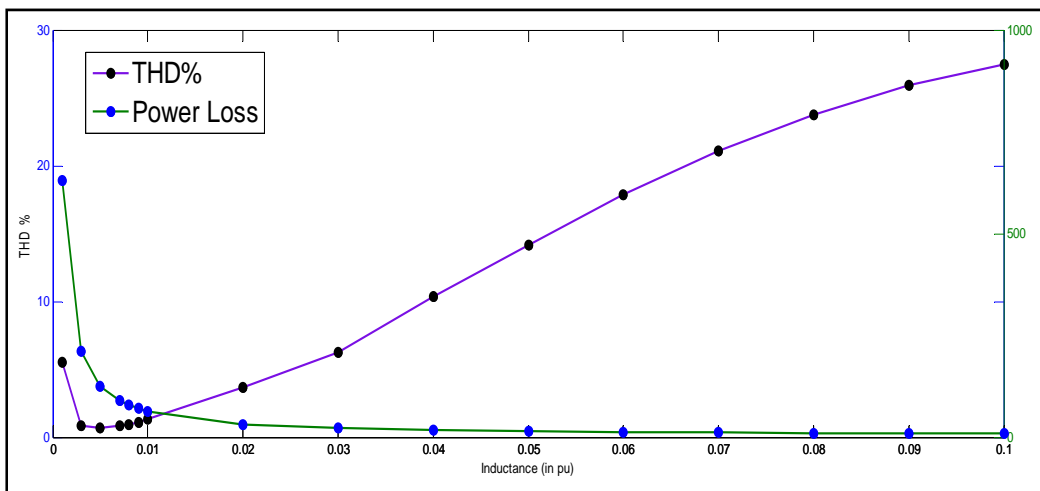


Fig.5.1 Variation of total power losses with L in p.u.

TABLE 5.5.Total losses with THD% variation

Inductance (L) in p.u.	Total losses of filter	THD%
0.01	65.2635	4.75
0.02	33.0045	1.39
0.03	22.5132	2.48
0.04	17.3560	5.13
0.05	14.2285	7.59
0.06	12.2365	9.69
0.07	11.3205	11.56
0.08	10.2215	13.12
0.09	9.0925	14.43
0.1	8.5975	15.88

Table 5.4 gives the total losses in the filter. With the increase in inductor value, it is observed that losses at fundamental frequency tend to increase whereas at switching frequency the losses are reduced. From the above graph an inductor value of 0.02 pu has lower THD% and at the same time lower losses. But previously we found out that $L \geq 4.875mH$ and also the power losses tend to decrease with increase in L, but this is limited by the THD%. We cannot increase the value of L where its THD% increases over 5%. Therefore the inductor value should be less than 19mH where the THD% is 5.13 as per TABLE 5.5. So considering both the factors we therefore the optimal values are $L= 4.875mH$, $C= 0.149mF$ and $R=5.7199ohm$ and with THD% of 3.2%.Now different switching methods are studied for inverter with the filter. The values of filter are taken as derived from the above procedure.

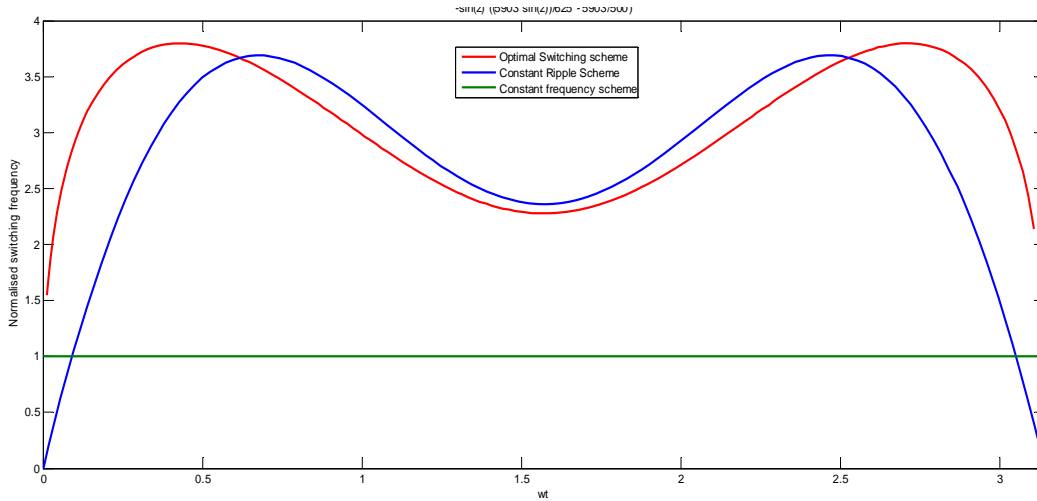


Fig.5.2. Normalised switching frequency

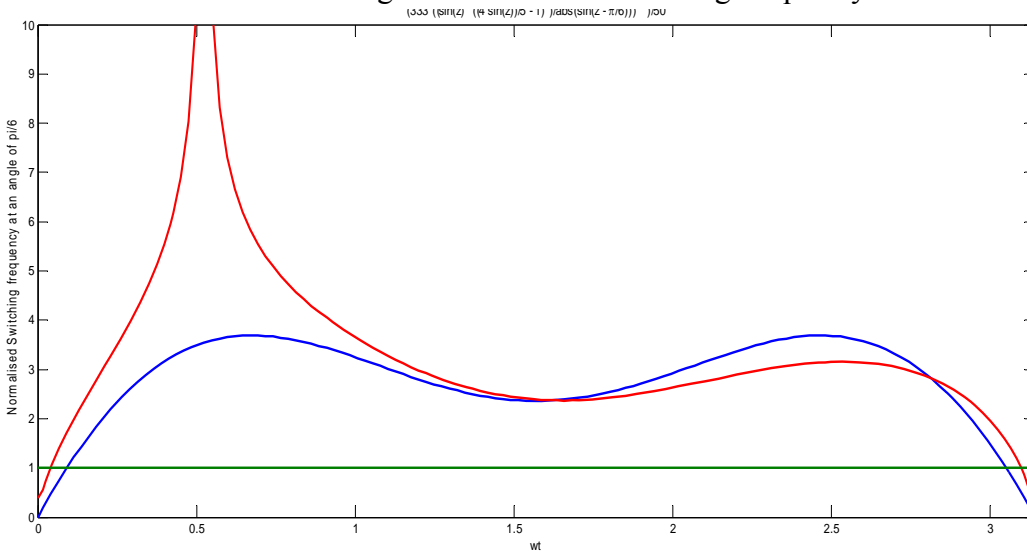


Fig.5.3. Normalised switching frequency at $\phi = \frac{\pi}{6}$

Above two plots are for normalized switching frequency for all the three methods. For all the methods, the parameters like DC input voltage, modulation index are taken same. Fig.5.2. shows the plot where $\phi = 0$ whereas Fig.5.3. is of $\phi = \frac{\pi}{6}$. When the switching frequency is compared to the current ripple at that moment is observed that in case of optimal switching scheme, switching frequency is higher when ripple is high and it is lower for smaller ripple. In the constant ripple scheme the switching frequency is directly proportional to the magnitude of ripple [7]. In the Fig. 5.3, it is observed that at certain angle the switching frequency has increased to an infinite value which is practically not possible. In this case the highest amount of switching frequency should be limited for the safety of equipment. Hence these changes in the

switching frequency results in the changes in switching losses which are further plotted in Fig.5.4. and Fig.5.5.respectively.

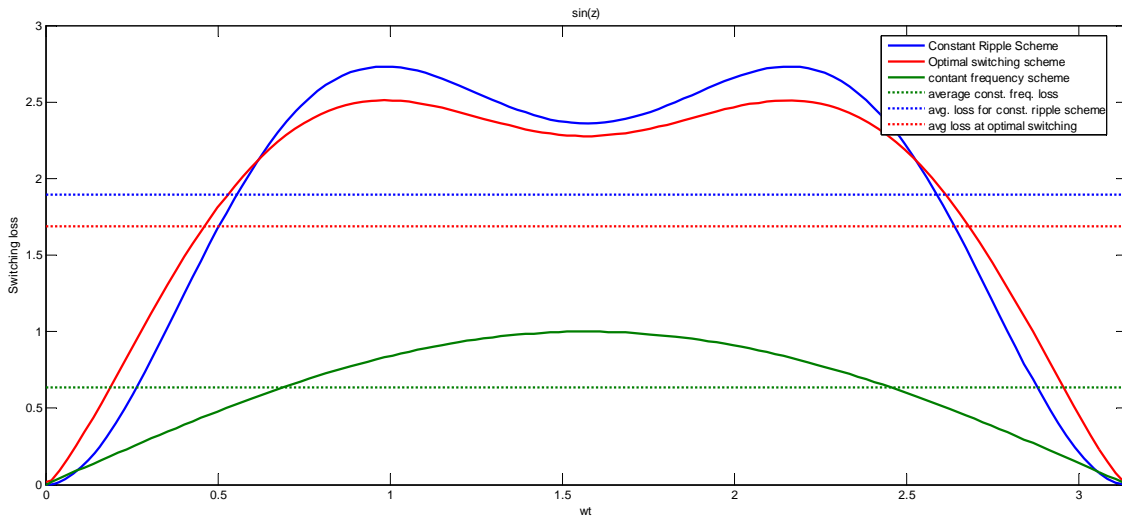


Fig.5.4.Switching loss and their average values for a cycle

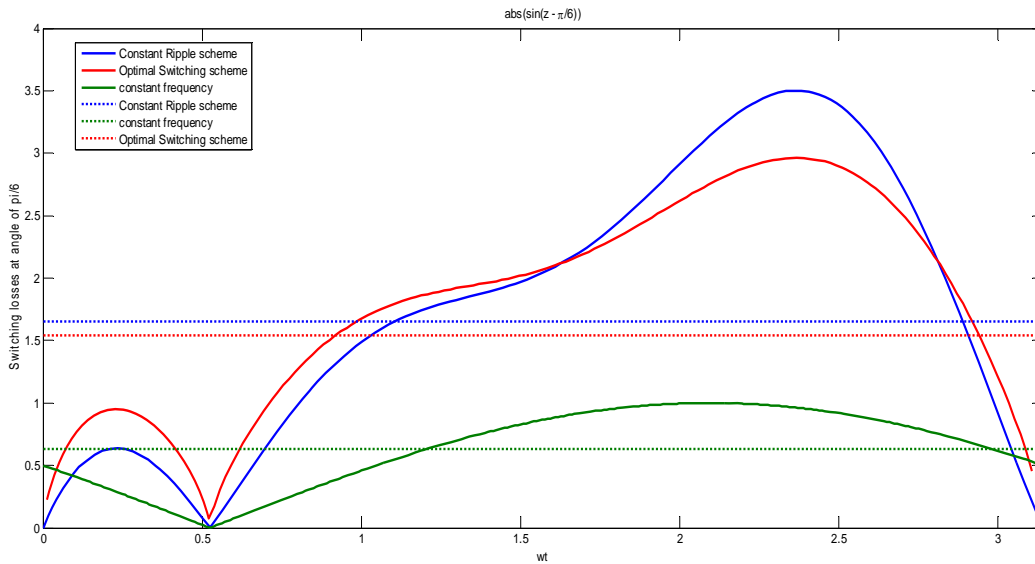


Fig.5.5. Switching loss and their average values at $\phi = \frac{\pi}{6}$

The average is switching losses plotted above proves that the losses for constant switching is lower than that of from constant ripple scheme and optimal switching scheme. It is observed though the optimal switching scheme has higher switching losses at some period; it has lower losses at peak values. In the case where $\phi = \frac{\pi}{6}$, there more reduction losses compared to constant ripple losses at peak values.

CHAPTER 6

Conclusions and Future work

6.1 CONCLUSIONS:

In this project the optimal design of LCL filter and switching loss reduction in grid connected inverter system is studied. From the study, the following observations are made. LCL filter can provide good grid synchronization without knowledge of grid impedance. Furthermore, The RMS calculation of the switching ripple current can be used for loss calculation of grid-connected single-phase inverter systems. The agreement with the simulation results to a prodigious extent with a good sinusoidal current, a lesser harmonic component is obtained. An optimal LCL filter design along with switching loss reduction is done. Hence, the optimal filter is designed considering THD% and ripple factor. And for that value of inductor different switching losses are studied. It is found that for grid connected system where switching of inverter is very low, constant switching scheme has much lower losses compared to the other two methods. But, during load variation there would be variation in switching frequency and hence constant frequency cannot be maintained. In order overcome this draw back one can employ adaptive hysteresis control in the inner feedback control loop which is also called constant ripple scheme. However, it is found that optimal switching scheme gives lesser switching losses and maintaining of constant switching frequency is beyond the scope of this project.

6.2 FUTURE WORK:

Further this work can be continued simulating the closed loop response and improving the whole performance of the system. Also now-a-days active damping is also applied for grid connected applications, which provide lesser filter without resonance problem.

REFERENCES

- [1] M. Singh, V. Khadkikar, A. Chandra, R.K. Varma, "Grid interconnection of Renewable Energy sources at the distribution level with power quality improvement features," *IEEE Transactions on Power Delivery*, vol.26, no.1, pp.307-315, Jan. 2011.
- [2] F.Blaabjerg, Z. Chen, and S. B. Kjaer, "Power Electronics as Efficient Interface in Dispersed Power Generation Systems," *IEEE Trans., Power Electron.*, vol. 19, no. 5, pp. 1184–1194, Sep. 2004.
- [3] Hanju Cha, T.K. Vu, "Comparative Analysis of Low-pass Output Filter for Single-phase Grid-connected Photovoltaic Inverter," Proc. of *IEEE Applied Power Electronics Conference and Exposition*, 2010, pp. 1659-1665.
- [4] Yaosuo Xue; Liuchen Chang, Sren Baekhj Kjaer, J. Bordonau; T. Shimizu, "Topologies of single-phase inverter for small distributed power generators: an overview", *IEEE Transactions on Power Electronics*, vol. 19, pp 1305–1314.
- [5] Hyosung Kim, Kyoung-Hwan Kim, "Filter design for grid connected PV inverters", Proc. of IEEE International Conference on Sustainable Energy Technologies, ICSET200), pp.1070-1075, 2008.
- [6] Parikshith.B.C, Dr.Vinod John,"Higher order output filter design for grid connected Power Converters," Proc. of Fifteenth National Power Systems Conference NPSC 2008, IIT Bombay, December 2008.
- [7] L Umanand,"Power Electronics: Essentials & Applications", Wiley Publications, 2009. First Edition.
- [8] Blaabjerg, F.; Teodorescu, R.; Liserre, M.; Timbus, A.V., "Overview of Control and Grid Synchronization for Distributed Power Generation Systems" *IEEE Transactions on Industrial Electronics*, Vol.:53 ,Issue:5,2006 , Page(s): 1398 – 1409.
- [9] Lingrong Zeng, Liuchen Chang, "Improved Current controller Based on SVPWM for Three-Phase Grid-Connected Voltage Source Inverters" Proc. of IEEE PESC '05. Page(s): 2912 – 2917.
- [10] Lingrong Zeng, Liuchen Chang, "Improved Current controller Based on SVPWM for Three-Phase Grid-Connected Voltage Source Inverters" Proc. of IEEE PESC '05. Page(s): 2912 – 2917.
- [11] E.Twining and D. G. Holmes, "Grid current regulation of a three-phase voltage source inverter with an LCL input filter," *IEEE Trans. Power Electron.*, vol. 18, no. 3, pp. 888–895, May 2003.
- [12] Cannegowda, P.; John, V.; , "Filter Optimization for Grid Interactive Voltage Source Inverters," *Industrial Electronics, IEEE Transactions on* , vol.57, no.12, pp.4106-4114, Dec. 2010.
- [13] Xiaolin Mao; Ayyanar, R.; Krishnamurthy, H.K.; , "Optimal Variable Switching Frequency Scheme for Reducing Switching Loss in Single-Phase Inverters Based on Time-Domain Ripple Analysis," *Power Electronics, IEEE Transactions on* , vol.24, no.4, pp.991-1001, April 2009.
- [14] J.W.Kolar, H. Ertl, and F.C. Zach, "Influence of the modulation method on the conduction and switching losses of a PWM converter system," *IEEE Trans. Ind. Appl.* ,vol.27,no.6,pp. 1063-1075, Nov./Dec. 1991.

- [15] Hyosung Kim, Kyoung-Hwan Kim, "Filter design for grid connected PV inverters", IEEE International Conference on Sustainable Energy Technologies (ICSET2008), pp. 1070-1075, 2008.
- [16] R.Ortega, E. Figueres, G.Garcera, C.L. Trujillo, D.Velasco, "Control techniques for reduction of the total harmonic distortion in voltage applied to a single phase inverter with non linear loads: Review," Renewable and Sustainable Energy Reviews 16(2012) 1754-1761.

APPENDIX

A. SMALL SIGNAL OF SINGLE PHASE VSI:

Case 1:

When switches S1 and S2 are ON the resulting circuit will be as shown in Fig.A.1.

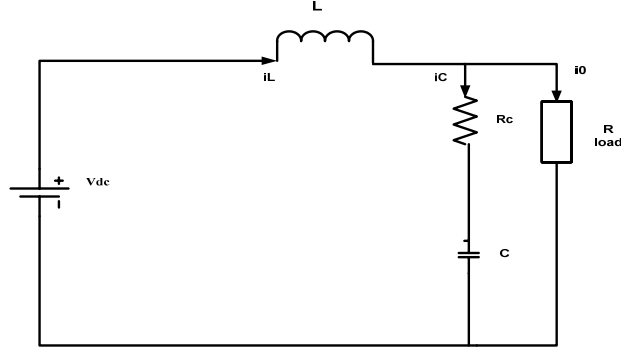


Fig.A.1. when S1 and S2 switches are ON

The calculations of small signal modeling are adopted from [15]. Applying KVL in the above circuit

$$L \frac{di_L}{dt} = V_{dc} - V_0 \quad (\text{A.1})$$

and

$$i_C = i_L - i_0 \quad (\text{A.2})$$

$$C \frac{dV_C}{dt} = i_L - \frac{V_0}{R} \quad (\text{A.3})$$

Case 2:

When switches S3 and S4 are ON, the resulting circuit will be fig.A.2.

By applying KVL in the above circuit,

$$L \frac{di_L}{dt} = V_0 - V_{dc} \quad (\text{A.4})$$

And

$$i_C = -i_L - i_0 \quad (\text{A.5})$$

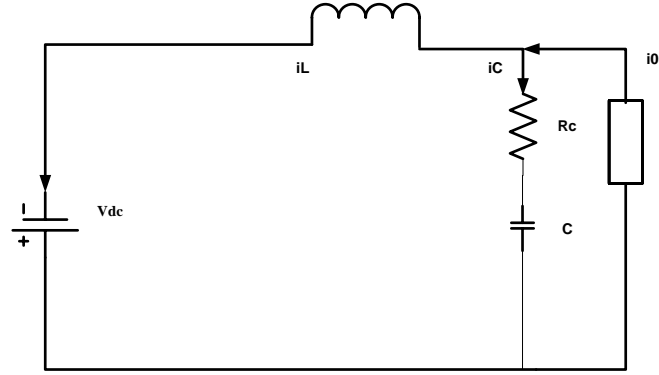


Fig.A.2. when switches S3 and S4 are ON

$$C \frac{dV_c}{dt} = -i_L - \frac{v_o}{R} \quad (A.6)$$

Let's consider average value of the inductor current and capacitor voltage over a switching period T_s .

$$L \frac{d\langle i_L \rangle_{T_s}}{dt} = d \cdot \langle V_{dc} - V_0 \rangle_{T_s} + d' \cdot \langle V_0 - V_{dc} \rangle_{T_s} \quad (A.7)$$

Where d = duty cycle, and $d'=1-d$

And

$$C \frac{d\langle V_c \rangle_{T_s}}{dt} = d \cdot \left\langle i_L - \frac{V_0}{R} \right\rangle_{T_s} + d' \cdot \left\langle i_L - \frac{V_0}{R} \right\rangle_{T_s} \quad (A.8)$$

Lets define an operating point as follows

Duty cycle = D

Input Voltage = V_{dc}

Output Voltage = V_0

Capacitor Voltage = V_C

Inductor current = I_L

Source current = I_s

In order to design a small signal model we will have to consider a small perturbation along with its steady state values

$$\langle V_{dc} \rangle_{T_s} = V_{dc} + v_{dc}$$

$$\langle V_0 \rangle_{T_s} = V_0 + v_0$$

$$\langle D \rangle_{T_s} = D + d$$

$$\langle I_L \rangle_{T_s} = I_L + i_L$$

$$\langle V_C \rangle_{T_s} = V_C + v_C$$

Putting above values in equation (A.7) and (A.8)

$$L \frac{dI_L}{dt} = D + d * V_{dc} + v_{dc} - V_0 - v_0 + 1 - D - d * -V_{dc} - v_{dc} + V_0 + v_0 \quad (A.9)$$

On simplification, the equation (A.9) gives rise to multiplication of steady state value terms along with linear and non linear terms. Multiplication of perturbation terms can be neglected as its results are very small. So resulting expression would be

$$L \frac{dI_L}{dt} = D - D'v_{dc} - D - D'v_0 + 2V_0d = (2D - 1)v_{dc} - 2d - 1v_0 + 2V_{dc}d \quad (A.10)$$

Similarly,

$$C \frac{dV_C}{dt} = (2D - 1)i_L - \frac{V_0}{R} + 2I_Ld \quad (A.11)$$

The resulting small signal model will be fig.A.3.

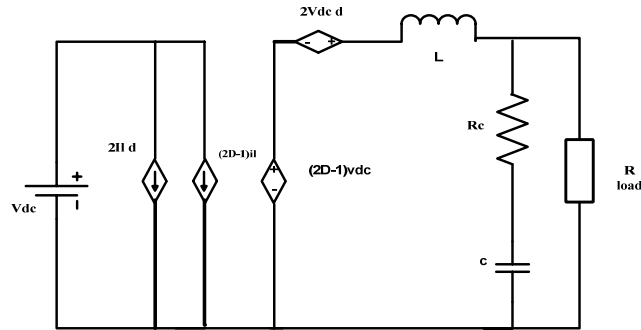


Fig.A.3. small signal model

B. INDUCTOR FILTER DESIGN:

Relationship between flux, mmf and permeance is [7].

$$\phi = \Lambda.N.i \quad (\text{B.1})$$

Differentiating the above equation and multiplying with N

$$N \frac{d\phi}{dt} = \Lambda.N^2 \frac{di}{dt} \quad (\text{B.2})$$

$$e = \Lambda.N^2 \frac{di}{dt} = L \frac{di}{dt} \quad (\text{B.3})$$

$$L = \Lambda.N^2 = \frac{\mu_o \mu_r A_c N^2}{l_m} \quad (\text{B.4})$$

As we know inductor is used as an energy storing device, therefore,

$$E_l = \frac{1}{2} Li^2 = \frac{1}{2} L \left(\frac{mmf}{N} \right)^2 = \frac{1}{2} \Lambda.mmf^2 \quad (\text{B.5})$$

An air gap is generally introduced for inductive applications wherein the core needs to store energy which is known as fringing model [5, 6].

$$\rho = \frac{l_m}{\mu_o \mu_r A_c} + \frac{l_g}{\mu_o A_c} = \frac{1}{\mu_o A_c} \left(\frac{l_m}{\mu_r} + l_g \right) \quad (\text{B.6})$$

$$I_f = \frac{KVA}{3 \times 0.9 \times V} \quad E_l = |I_f \times j2\pi f L| \quad (\text{B.7})$$

$$A_p = A_w A_c = \frac{2E_l}{K_w K_c J B_m} \quad (\text{B.8})$$

$$\Lambda = \frac{\mu_o \mu_r A_c}{l_m + \mu_r l_g} \quad (\text{B.9})$$

$$N = \sqrt{\frac{L}{\Lambda}} \quad a = \frac{I_{rms}}{J} \tag{B.10}$$

According to the values of l_m and A_p the core is selected and the inductor is designed.

PAPERS PUBLISHED

1. Debati Marandi, Naga Sowmya Tontepu, B.Chitti Babu, " Comparative Study between Unipolar and Bipolar Switching Scheme with LCL Filter for Single-Phase Grid Connected Inverter System", *In Proc. IEEE Students' Conference on Electrical, Electronics and Computer Sciences 2012 (SCEECS 2012)*, MANIT, Bhopal, Mar/2012-
Received Best Paper Award
2. Naga Sowmya Tontepu, Debati Marandi, B.Chitti Babu, " Optimal filter design and Switching loss reduction in grid connected inverter system", *In Proc. IEEE 2nd Students' Conference on Engineering and Systems 2013 (SCES 2013)*, MNNIT, Allahabad, Apr/2013.
3. Debati Marandi, Naga Sowmya Tontepu, B.Chitti Babu, "LCL Filter Response of 1- Φ Grid Interactive Inverter using Small Signal Modelling", *In Proc. IEEE Sponsored 1st National Conference on Power Electronics Systems & Applications (PESA 2013)*, NIT, Rourkela, pp.181-184, March/2013.